

Study on behavior of soil reinforcing pile in piled raft systems

M. Haghbin^{1,*}

Received: April 2014, Revised: June 2014, Accepted: October 2014

Abstract

This research examines the behavior of soil-reinforced piles and applied loads based on the analytical method and by using the numerical results of FLAC3D software for comparison with the analytical results. The analysis was based on a method called virtual retaining wall, the following into consideration: an imaginary retaining wall that passes the footing edge; the bearing capacity of footing on reinforced soil with piles, which was determined by applying equilibrium between active and passive forces on virtual wall; and a pile row that exists beneath the shallow foundation. To calculate the lateral pile resistance here, an analytical equation was then required. The main objective of this paper is to determine the percentage of applied load on pile. Similarly, the effect of adding pile in various positions relative to the present footing (underpinning) was studied in this research. The various parameters of this study included pile length, vertical distance of pile head to shallow footing, pile distance to center of footing and location of the pile. Finally, the findings were compared with the numerical results of FLAC3D and the formerly presented experimental results. Results show that the analytical method, while being close to other methods is more conservative.

Keywords: Location, Pile, Applied load on pile, Footing.

1. Introduction

Inevitable construction on a ground with various resistance calls for a variety of methods, such as layer reinforcement, cement and stone column injections, and resistance through pile use, to allow for soil improvement, rising soil strength, and reducing soil settlement.

Fig. 1 shows a pile with a shallow foundation was used to support a high structure load with inadequate soil resistance. Applied load on a pile depends on its location with respect to its foundation, pile and footing properties, and shallow foundation. It is notable that pile as soil reinforcement was also used for seismic retrofit and higher resistance of present footing (underpinning).

What had been considered in previous research was the bearing capacity of footing with pile group [1]. In fact, one of the effective ways to increase the footing bearing capacity is using pile foundation. However, an economical design of the project necessitated determining the exact contribution of applied load on pile and shallow foundation [2, 3]. The research findings revealed that footing and pile combination decreases settlement remarkably [4]. Previous researchers reported that the effect of pile and footing combination on reducing settlement is more than the increasing bearing capacity [5, 6].

Pile effect as soil reinforcement was studied on load-settlement curve [7].

Poulos and David reported a case study of Dubai's Twin Tower in which the disagreement between measured and predicted settlements was calculated by the boundary element method [8]. Using fully rigid raft, Thaher and Jesberger investigated the behavior of a vertically loaded pile-raft foundation by centrifuge modeling on over consolidated saturated clay [9]. By a fully flexible raft on stiff clay, Horikoshi and Randolph examined pile-raft foundation through a centrifuge physical model [10]. Poulos and Davis proposed a simplified analytical method named PDR with the assumptions of rigid cap and soil linear behavior [11].

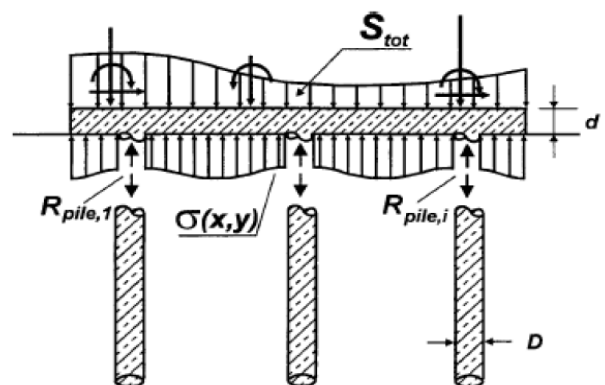


Fig. 1 Interaction between pile, soil and foundation

* Corresponding author: haghbin@iaua.ac.ir
 1 Assistant Professor, Department of Civil Engineering,
 Islamshahr Branch, Islamic Azad University, Islamshahr, Iran

Some research on the behavior of pile and footing combinations were presented using the finite element method [12-19]. Baziar et. al. (2009) compared numerical and experimental methods to model pile and footing combinations. According to their findings, load-settlement behavior of the combination with pile and footing is linear up until the applied load becomes less than the service load. Fig. 2 depicts the sample results of this study [19].

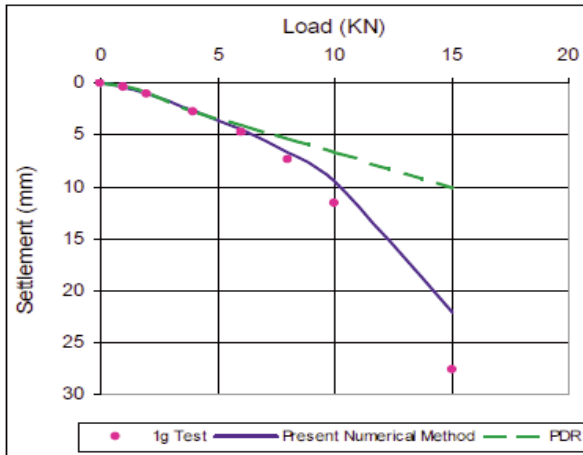


Fig. 2 Comparing of behavior of pile and footing combination with numerical and experimental methods [12]

Many researchers have determined the optimal design of pile and footing combination. Cooke et. al. (1986) reported that 30 percent of total load is applied on footing [20]. Hemsley (2000) reported that pile and footing tolerates 50 percent of applied load each with the assumption of a very high safety factor. Results indicated that disconnected piles to footing tolerate more loads than the connected ones [21]. Also, Cao et. al. (2004) made an experimental model of pile and footing combination, and studied the effect of various parameters such as pile length, number of piles, and thickness of footing on settlement [22]. Similarly, other researchers reported optimal design of pile and footing combination [23, 24]. Eslami et. al. (2012) reported the finite element method to determine the optimal design of pile and footing combination when piles are either disconnected or connected to footing [25]. Underpinning has been considered to be a useful method for seismic retrofit and for the improvement of existing footing. This method allows for an increase in bearing capacity of existing footing through the addition of piles beneath and around the existing footing, and determines the exact effect of the piles. Nonetheless, underpinning was subject to scrutiny by several researchers [26, 27].

Few studies have been carried out on the effects of the reinforcing pile position (beneath or around footing), the vertical distance of pile head to footing, pile length, and the type of soil on percentage of the applied load. The present paper addresses the effects of these parameters through use of the analytical method.

The behavior of disconnected reinforcing piles to footing and their effective factors was investigated in this study based on the analytical method of programming in

MATLAB software. This software was also used to compare numerical and analytical results. The analytical method was based on the virtual retaining wall method, in which an imaginary retaining wall was assumed to pass the footing edge. The bearing capacity of footing on reinforced soil was determined by the equilibrium between active and passive forces on the wall. A row of pile was assumed beneath the strip footing. Therefore, analytical equation was required to calculate the lateral pile resistance presented in this study. The main objective of this paper was to determine the percentage of applied load on pile and reducing settlement. Experimental results presented by other researchers were used to verify the analytical method. The varied parameters in this study included pile length, vertical distance of pile head to shallow footing, pile distance to footing center, and location of pile relative to footing.

2. Research Method

Analytical and numerical methods were used here in order to study the behavior of soil reinforcing pile and the effective factors on it. Analytical method was based on the virtual retaining wall and results were presented with the MATLAB programming software. This method was reported to determine bearing capacity of footing on flat ground [28]. Numerical analysis was also presented by modeling it in FLAC3D software. In the analytical method based on soil allowable resistance, an imaginary retaining wall was assumed to pass the strip footing edge in order to calculate the bearing capacity of footing. As seen in Fig. 3, this wall tolerates active force P_a due to the footing loading and the soil beneath the footing. The surrounding soil was in passive condition as it exerted force P_p on the wall. Under the unreinforced soil, the values of P_a and P_p were computed using the following equations with the Coulomb lateral earth pressure method (Fig. 3):

$$P_a = q_{ult}K_a H_1 \cos \delta + \frac{1}{2} K_a \gamma (1 - k) H_1^2 \cos \delta - c K_{ac} H_1 \cos \delta \quad (1)$$

$$P_p = \frac{1}{2} K_p \gamma (1 - k) H_1^2 \cos \delta + c K_{pc} H_1 \cos \delta + K_p \gamma (1 - k) D H_1 \cos \delta \quad (2)$$

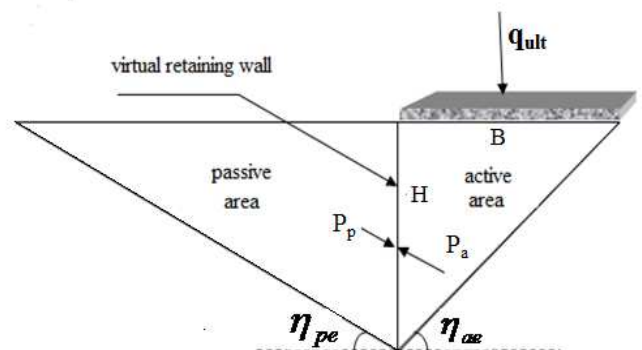


Fig. 3 Failure surface of soil beneath the strip footing with virtual retaining wall method

Finally, bearing capacity of strip footing was determined by applying equilibrium between active and 2

$$q_{ult} = \left(\frac{1}{2} K_p \gamma (1-k) H_1^2 \cos \delta + c K_{pc} H_1 \cos \delta + K_p (1-k) \gamma D H_1 \cos \delta - \frac{1}{2} K_a \gamma (1-k) H_1^2 \cos \delta + c K_{ac} H_1 \cos \delta \right) \left(\frac{1}{K_a H_1 \cos \delta} \right) \quad (3)$$

where K_a, K_p : active and passive coefficients (Coulomb method), H_1 : height of virtual wall and it is equal to $B \tan(\eta_{ae})$, δ : friction between soil and wall, γ : specific density of soil, C : soil cohesion, K : vertical seismic coefficient, D : depth of foundation, K_{ac}, K_{pc} : cohesion coefficient of active and passive, η_{ae}, η_{pe} :

seismic bearing capacity. As shown in Fig. 3, the angles of active and passive areas with horizontal direction (Coulomb method). Also, friction angle of soil affects these two angles remarkably and with increasing friction angle of soil η_{pe} increases and η_{ae} decreases.

Eq. (3) could be written as the following equation:

$$q_{ult} = c N_c + \gamma D N_q + 0.5 \gamma B N_\gamma \quad (4)$$

$$\text{where } N_q = \frac{K_p (1-k)}{K_a}, \quad N_c = \frac{K_{pc} + K_{ac}}{K_a}, \\ N_\gamma = \frac{\tan(\eta_{ae})}{K_a} (1-k) (K_p - K_a)$$

With pile-reinforced soil beneath the footing bearing capacity of the strip footing was found by the virtual retaining wall method. The percentage of applied load on piles was then calculated, which in turn required for the lateral pile force applied on virtual wall be determined. The Location of reinforcing piles of soil in active and passive areas, and pile length in failure surface affected both the pile resistance and the applied force on virtual wall. Therefore, in the next section, an analytical equation is presented to determine the lateral resistance of reinforcing pile on soil.

2.1. Lateral resistance of reinforcing pile

Lateral resistance of pile had to be calculated in order to determine the effect of reinforcing pile on bearing capacity of the piled raft system. For purposes of this research, lateral resistance of the passive pile was determined by simulating the piles as wall, and by adding shear resistance to the soil surrounding the piles. The presented method was used to calculate active pile resistance against external load in cohesion-less soil. The validity of this method was verified by results obtained from centrifuge tests [29]. Therefore, the following equation was presented to determine the passive pile lateral resistance. It is notable that soil plastic deformation between piles in a row affects the piles' lateral resistance

passive forces:

and power of passive coefficients (K_p, K_{pc}), as shown in the method below:

$$p_u = (\eta K_p^2 \gamma z + \eta K_{pc}^2 c) b + (\xi K \gamma z \tan \delta) b \quad (5)$$

where η, ξ : shape factor, K : lateral pressure of soil coefficient, δ : friction between soil and pile, z : depth, K_{pc} : cohesion coefficient of passive soil and K_p : passive coefficient. K_p and K_{pc} are calculated with Coulomb method, b : pile diameter.

In fact, the power of passive coefficients indicates the effect of combining soil plastic deformation between piles in a row and pile resistance, which varies depending on different spacing of piles in a row. As a result, the power of K_p and K_{pc} equals to 2 (Eq. (5)) when the ratio of piles spacing in a row to pile diameter becomes a minimum ($S_1/b=2.5$). Also, when $S_1/b=8$, the power of passive coefficients equals 1, and the soil plastic deformation between piles does not affect pile lateral resistance. Similarly, the effect of piles spacing in a row on soil plastic deformation between piles was obtained by Wei et.al using FLAC3D software as well as Ito and Matsui's [30, 31]. The effect of seismic coefficient on lateral pile resistance is included in the soil passive pressure coefficient.

Results indicated that the results of analytical equation for determining pile lateral resistance are compatible with those of previous researches, i.e. the Ito-Matsui method. Ito and Matsui (1975) presented a method to calculate lateral pressures on piles passively located in a plastically deforming ground while considering the soil squeeze between the piles (Fig. 4). Ito and Matsui (1975) considered two types of plastic states in the ground surrounding the passive pile [31]. In fact, this method calculates the total force applied on piles and the soil between piles, and then subtracted the applied force on the soil between piles from total force. Afterwards, the force applied on each pile is determined (Fig. 4). Ito and Matsui method has limited assumptions, and is valid only for rigid piles, one-pile rows, and fixed piles in stable layers. It is unable to consider the effect of earth slope and seismic loading. The presented method remedies these limiting assumptions for determination of passive pile resistance. Previous studies confirmed the results obtained from Ito and Matsui method when its assumptions were available with field data [23]. Therefore, Ito and Matsui method is used to indicate the validity of the suggested method.

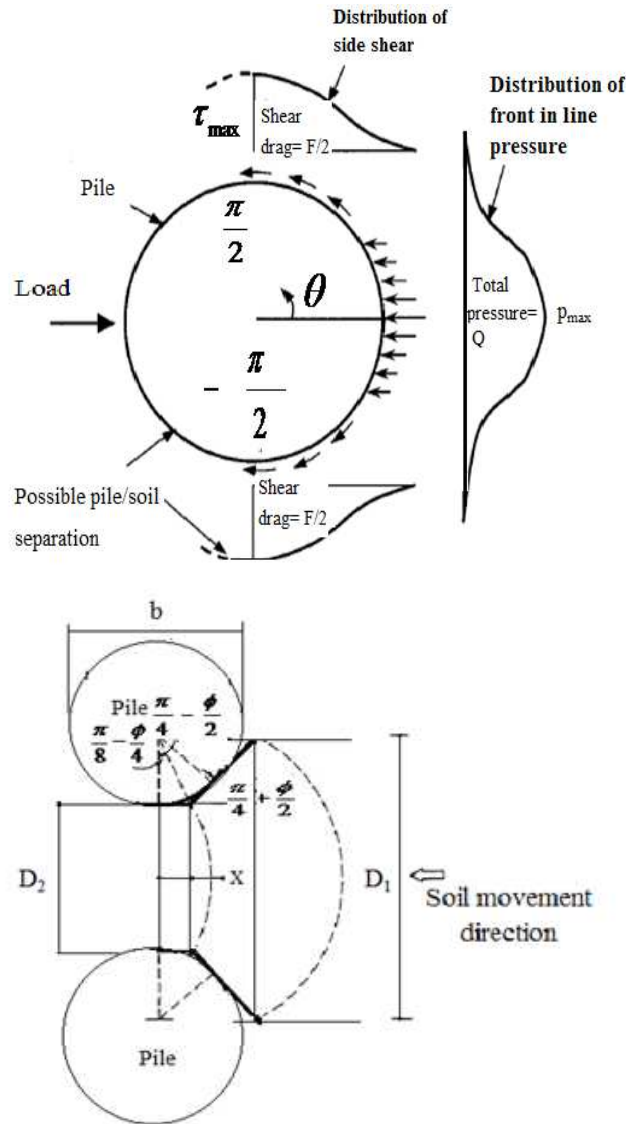


Fig. 4 Lateral resistance of soil around piles

2.2. Bearing capacity of footing on reinforced soil with piles

In this section, bearing capacity of strip footing on reinforced soil with pile was determined through the virtual retaining wall method and the lateral pile resistance equation. Reinforcing piles of soil were assumed to be installed beneath and around the footing, which means piles were installed in both active and passive areas. The following equation was used to determine the bearing capacity of footing on reinforced soil with piles:

$$q_{ult} = \left(\frac{1}{2} K_p \gamma H_1^2 \cos \delta + c K_{pc} H_1 \cos \delta + K_p \gamma (1-k) D H_1 \cos \delta - \frac{1}{2} K_a \gamma H_1^2 \cos \delta + c K_{ac} H_1 \cos \delta + F_{pa} + F_{pp}\right) \left(\frac{1}{K_a H_1 \cos \delta}\right) \quad (6)$$

where F_{pa} , F_{pp} : lateral force of pile in active and passive areas, determined with Eq. (5) (Fig. 5).

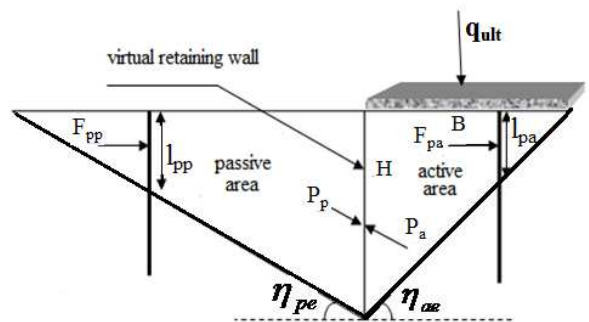


Fig. 5 Failure mechanism in reinforced soil with piles

Eq. (6) could be written as following equation:

$$q_{ult} = c N_c + \gamma D N_q + 0.5 \gamma B N_\gamma + \frac{F_{pa} + F_{pp}}{K_a B \tan \eta_{ae} \cos \delta} \quad (7)$$

In the following equation, applied load on piles with respect to bearing capacity of a piled raft system (Eq. 7) is presented:

$$\alpha = \frac{q_p}{q_{ult}} * 100 \quad (8)$$

Where q_p is determined with following equation:

$$q_p = \frac{F_{pa} + F_{pp}}{K_a B \tan \eta_{ae} \cos \delta} \quad (9)$$

Eq. 8 illustrates the effect of various parameters on the percentage of applied load on reinforcing pile or reducing settlement. The applied load on the pile reduced the load on raft, and it was proportional with the settlement.

2.3.3 D modeling in FLAC3D software

The FLAC-3D software was used to investigate a suitable analysis approach based on the finite difference method. In order to set up the numerical model and to carry on a simulation, three fundamental components of the finite difference approach should be specified including grid geometry, boundary and initial condition and constitutive behavior. Fig. 6 illustrates the model in FLAC3D software. Solid elements were used to define the geometry of piles and raft. The procedure of geometric modeling was simplified using pre-shape zones. Solid zones were simply divided into several elements in order to generate grid or mesh.

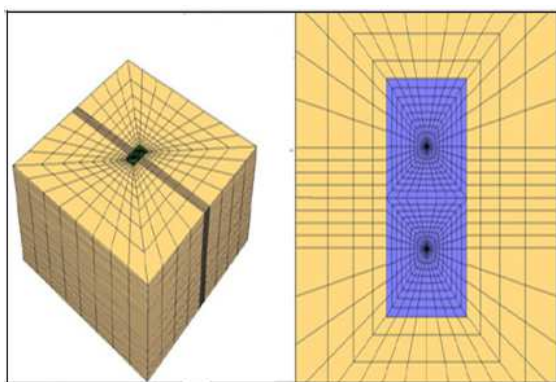


Fig. 6 Modeling in Flac3D software

Table 1 Properties of soil, pile and interface in FLAC 3D software

Interface		Pile		Soil	
2 ton/m ²	Cohesion	2.38e06 ton/m ²	Modulus of elasticity	2 ton/m ²	Soil cohesion
40	Friction angle of soil	0.15	Poisson's ratio	40	Friction angle of soil
10000 ton/m ²	K _n	1.13e06 ton/m ²	Bulk Modulus	0.3	Poisson's ratio
10000 ton/m ²	K _s	1.03e06 ton/m ²	Shear Modulus	Varies with depth	Modulus of elasticity

In most recently advanced numerical simulation of pile-raft, a complex constitutive model, similar to the cap model was used to present non-linearity of soil. Complex constitutive models require more soil parameters than simple constitutive models (i.e. Mohr- Coulomb) to define numerical simulation. Therefore, applying a complex constitutive model demands many efforts such as performing complex shear tests or back analyses in order to specify soil parameters. In the present research a simple constitutive model, Mohr-Coulomb elasto-plastic criteria was used for the medium sandy soil to overcome the mentioned difficulties. The main soil parameters used in the analysis are internal friction angle, cohesion coefficient(C), Young modulus (Es) and Poisson's ratio (ν_s). Table 1 indicates the properties of pile, footing and soil. Using the Mohr-Coulomb model may also reduce the analysis time in comparison with previous approaches with complex constitutive models. One of the main problems in numerical simulation of pile-raft is to model the contact between soil and foundation, including piles and raft. Since sliding is possible to occur on the contact zone, to present the real condition, it is necessary to implement interface elements on the contact zone. To consider soil-pile- footing interaction in FLAC3D software, interface elements was used around and at the end of piles, as well as beneath the footing that were in contact with the soil (Fig. 7). Before applying the load to the system, the model equilibrium under initial state was controlled. To simulate this condition, the model was simulated under initial stresses caused by gravity of soil. Models analysis continued until the unbalanced force on the nodes with the ratio of $1*10^{-5}$ was achieved. The lower the ratio, the more accurate the results were; while the analysis time increased.

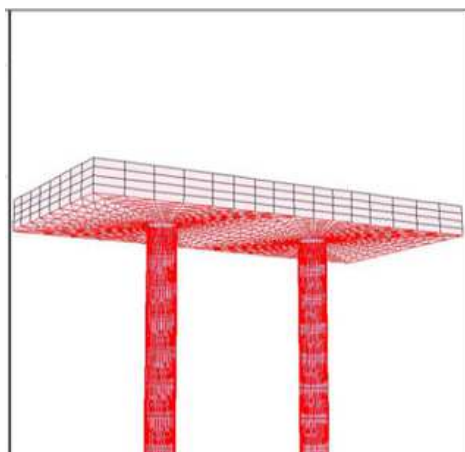


Fig. 7 Using interface elements around pile and footing

Modeling a footing with one row of pile was used in order to consider the effect of mentioned parameters. Soil size around pile and footing was increased until the error of output became negligible. A thickness of 0.5m was assumed for modeling the soil and reinforcing piles. Of course in all the models, the nodes of neighboring elements coincided precisely. It is notable that numerical results were obtained based on allowable settlement.

3. Results and Discussion

The effect of various parameters on percentage of the applied load on reinforcing pile of soil was determined by the analytical method and programming of MATLAB software. In the present study, center-to-center spacing of piles in a row was equal to 2.5b. First, the results of determining pile lateral resistance with the suggested method were compared with that of Ito and Matsui. Then, to test the accuracy of the presented method, results of the determining applied load on reinforcing pile with the analytical method were compared to the numerical results obtained from FLAC3D software and previous experimental results. Finally, the effect of various parameters on applied load on reinforcing pile was studied. The parameters discussed in this section included pile length, distance of pile head to shallow foundation, distance of pile to footing center, and the location of reinforcing pile in active and passive areas (underpinning).

3.1. Comparison of suggested method to determine lateral resistance of pile with Ito and Matsui method

In this section, the presented analytical method to determine pile lateral resistance was compared with Ito-Matsui's method [31]. One row of pile was assumed while the ratio of center-to-center spacing of piles to pile diameter is equal to 2.5. In fact, the maximum lateral resistance of one pile row is made in this distance because of plastic deformation of soil between piles. The power of passive coefficients was equal to 2, and sliding layer length was assumed 4 m. As shown in Fig. 8, results of the presented method and Ito and Matsui's were close, which indicates acceptability of the presented method. Based on

the results, any increase in soil friction angle will cause increase in pile lateral resistance, because soil friction angle affects the normal and shear resistance of soil around pile remarkably.

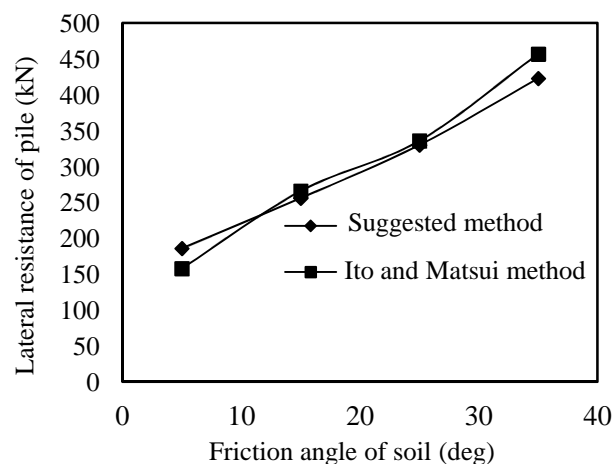


Fig. 8 Comparison of suggested method to determine lateral resistance of pile with Ito and Matsui method in various friction angles of soil

3.2. Comparison of analytical and numerical methods in present study

In this section, the presented analytical method of study that was based on allowable resistance of soil was compared with numerical results of FLAC3D software obtained upon allowable settlement. It is notable that in present study, a strip footing with a foundation width (B) equal to 2 m was investigated. The pile had been installed in the center of that foundation. Table 1 indicates the properties of pile, footing and soil. Fig. 9 illustrates results of the comparison, and the effect of pile length (l) on the applied load of reinforcing pile.

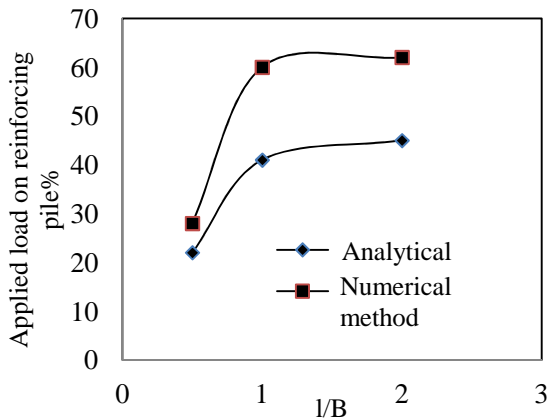


Fig. 9 Comparison of analytical method to determine effect of ratio of pile length to foundation width on applied load on reinforcing pile with numerical method

Results of the analytical method were less than the numerical method; Fig. 9 however, shows that the results of the two methods were almost close, and the analytical method presented in this study was acceptable. The figure also indicates that analytical results were more conservative than numerical ones. One reason for the different results lies in the various assumptions of numerical and analytical analysis. Besides, numerical results were obtained from allowable settlements, but analytical results were presented upon soil allowable resistance.

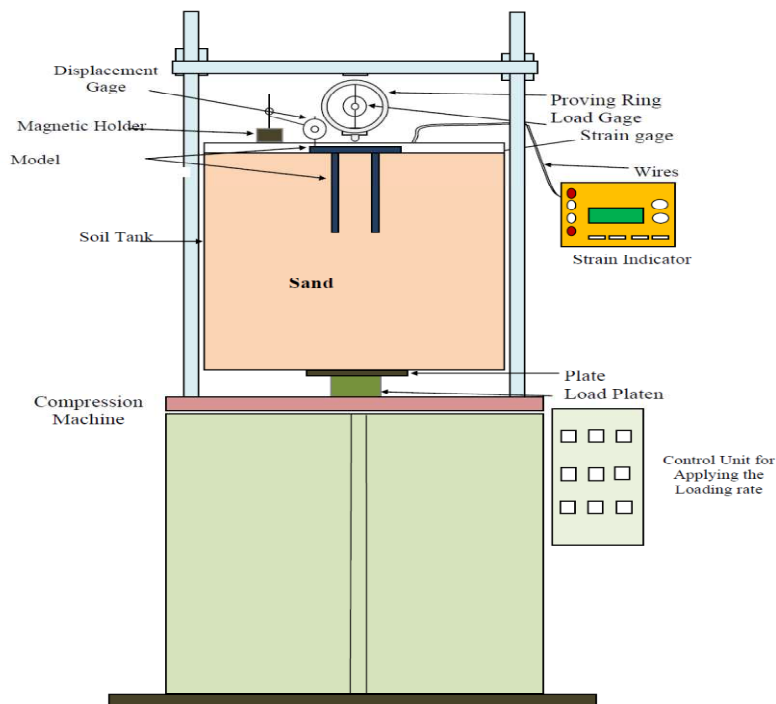


Fig. 10 Laboratory model [23]

Using parameters in the analytical equation of the present study (Eqs. 7, 8), the analytical method and the obtained percentage of the loaded pile was compared with the Fattah et.al experimental method. Of This study completes the analysis of shallow foundation for the 2*1 pile group by assuming a one pile row beneath the footing.

3.3. Comparison of analytical method with experimental results

In this section, the analytical results of the present study were compared with experimental results presented by Fattah, et. al (2011) and Baziar, et. al (2009) [19, 32]. Fig. 10 indicates that the assumed soil for the Fattah, et. al laboratory model is sand, and has a friction angle equal to 38 degrees. In this model, pile length was assumed constant and equal to 200 mm; pile diameter varies (9, 12, 15 mm); and foundation width is 6 cm. In Fattah's study, a small-scale "prototype" model was tested in a sand box with a load applied to the system through a compression machine. The settlement was measured at the center of the raft, strain gages were then used to measure the strains, and calculate the total load carried by the piles. The effects of pile length, diameter and raft thickness on the load carrying capacity of the piled raft system were included in the load-settlement presentation. Results show that the percentage of the load carried by piles to the total applied load of the groups (2*1, 3*1, 2*2, 3*2) with raft thickness of 5 mm, pile diameter of 9 mm, and pile length of 200 mm is 28%, 38%, 56%, 79%, respectively. The percentage of the load carried by piles increases with respect to the increase in piles.

In the laboratory model, the center-to-center spacing of piles in a row was constant and equal to 5 cm, while the pile diameter varied. Therefore, in the suggested method for determining pile lateral resistance, the power of passive coefficients increased by decreasing the ratio of center-to-center spacing between piles in a row to the pile diameter.

As seen in Table 2, the pile with analytical and experimental method under applied loads showed close and acceptable agreement.

Table 2 Piles capacity for the studied cases ($B=6\text{ cm}$)

Case	% of load carried by piles (Experimental results, Fattah, et al, 2011)	% of load carried by piles (Analytical results of present study)
(2*1) Group, $l=200\text{ mm}$, $b=9\text{ mm}$	30	27
(2*1) Group, $l=200\text{ mm}$, $b=12\text{ mm}$	39	38
(2*1) Group, $l=200\text{ mm}$, $b=15\text{ mm}$	52	48

The following section illustrates a comparison between the experimental results presented by Baziar, et.al and the analytical results of this study. The bearing -settlement behavior of combined pile-raft foundations on medium dense sand was investigated in the Baziar et.al experimental study, and a 1g physical model test was performed on a circular rigid raft underpinned with four model piles (Fig. 11). Findings in the Baziar et.al model revealed the numerical methods to be accurate as long as the applied load did not exceed the working load. The

numerical model however, proved efficient for loads even beyond the working load.

Laboratory tests were performed to measure the geotechnical parameters of medium sand used in the physical model test. Test results showed the internal friction, the cohesion coefficient, the Poisson's ratio and the average elastic modulus to be 38 degrees, 0.01 kPa, 0.25 and 12.5 MPa respectively. Pile and raft properties were indicated in Fig. 11. In the Baziar et.al study, the percentage of the load applied on the pile was determined through different loads (Fig. 12). However, our analytical method was used to illustrate the ultimate bearing capacity of the foundation system was found to be 15 kPa. Therefore, in the proposed method the applied load on pile was obtained when the load was at 15 kPa (Fig. 12). Results indicated that when the load was at 15 kPa, the percentage of the applied load on pile was equal to 30, 40, and 52 in all the suggested, experimental, and numerical methods respectively. In fact, the result of the analytical method was 10 percent less than that of the experimental method, indicating that the analytical results are more conservative than the experimental ones. It is notable that assumptions of the analytical method can cause a reduction in the applied load on pile with respect to the experimental method. Overall, results of various methods showed to be close and acceptable.

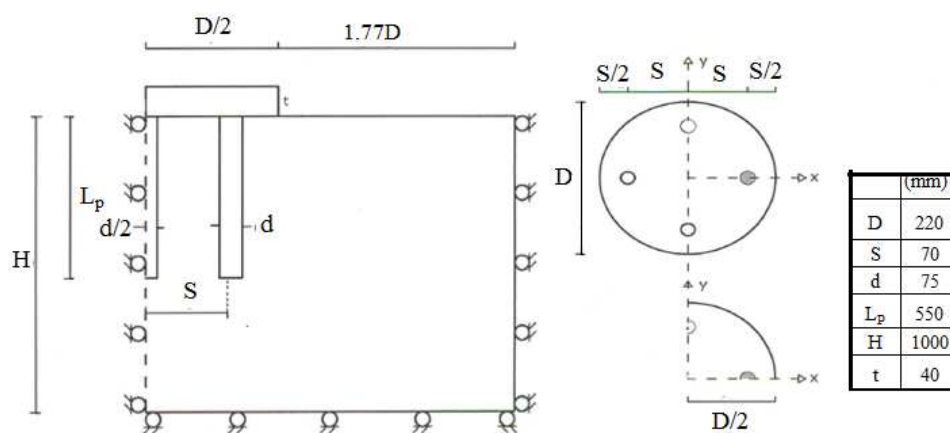


Fig. 11 Physical model geometry of Baziar et. al [12]

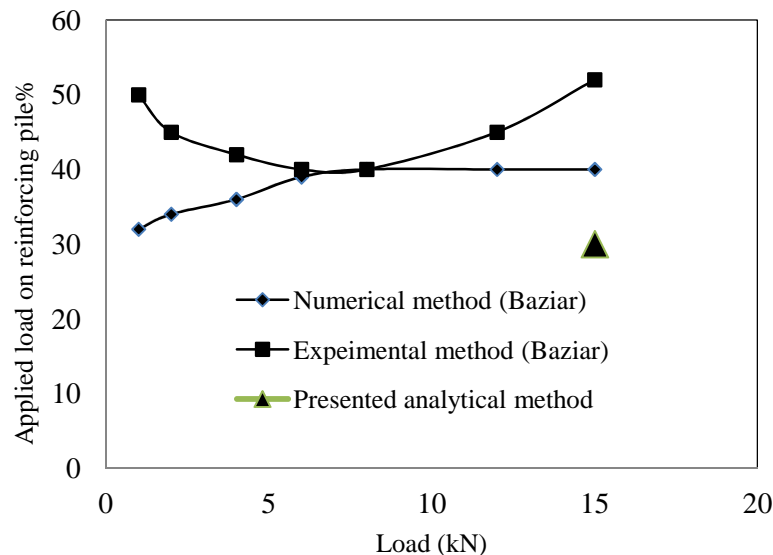


Fig. 12 Comparing suggested method with experimental and numerical method presented with Baziar, et. al to determine percent of applied load on pile

3.4. Parametric Studies

In order to do an optimal design of shallow foundation and pile-reinforced soil, it is essential to determine the contributions of pile and shallow foundation, as well their influential factors. Thus the effects of various parameters on the percentage of the applied load on pile (α) and its reducing settlement were studied. It should be noted that the settlement decreased with the percentage of applied load on pile because of the decrease in applied load on shallow foundation. Therefore, the applied load on pile and the settlement reduction had almost equal percentage. In present study, the following were assumed: a strip footing, foundation width (B) = 2 m, soil friction angle = 40 deg, cohesion less soil, ratio of pile length to foundation width (l/B) = 2, pile diameter (b) = 1 m, spacing of piles in a row (D_1) = 2.5 b , and pile locations in active and passive areas at the foundation center and edge.

3.4.1. Effect of pile length on behavior of reinforcing pile of soil

The effect of pile length (l) on the percentage of applied load on soil reinforcing pile was considered in this section. In present study, distance of pile head to shallow foundation (S) was 0. It is notable that pile location first affected pile length in failure surface, and then its lateral resistance. In other words, if the pile is installed beneath (active area) or around (passive area) the foundation, the pile length will vary depending on the failure surface made beneath the foundation, remarkably affecting the applied load on pile.

Initially, it was assumed the pile had been installed in the foundation center (active area). Fig. 13 depicts that any increase in the ratio of pile length to foundation width (l/B) elevates the applied load (α) on pile till $l/B = 1$, and

the percentage of the applied load on pile and its reducing settlement is approximately 62. In the case study, if l/B is greater than 1, the pile length does not affect the applied load, mainly because any increase in pile length in failure surface (when the pile does not pass the failure area) increases the percentage of applied load on pile. In present study, the pile passed the failure surface when its length equaled the foundation width. It caused the pile length in failure surface to become constant with no effect on the percentage of applied load on the pile.

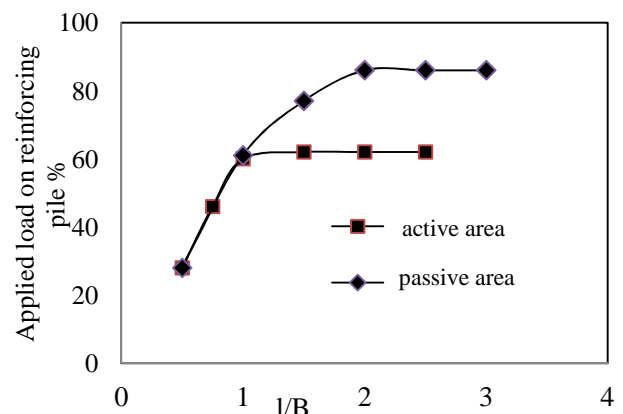


Fig. 13 Effect of pile length on percent of applied load on pile in active and passive area

According to the assumed failure surface of the virtual retaining wall method shown in Fig. 5, the failure surface angle in passive area is less than the one in active area, which leads to varied effects of pile length in these two areas. Fig. 13 shows that with the value of pile length as $2B$, the percentage of applied load on pile in passive area is maximized and equal to 86 percent. When pile length is over $2B$, it does not affect the percentage of applied load on pile, because the reinforcing pile passes failure surface and the pile length remains constant.

3.4.2. Effect of pile head distance from foundation on behavior of soil reinforcing pile

In this section, effects of the foundation's pile head distance to the foundation width (S/B), on the percentage of applied load on reinforcing pile was investigated. Pile length was assumed to be equal to $2B$. As shown in Fig. 14, location of the pile in active and passive areas affect reinforcing pile behavior with changing S/B . Results indicated that any increase in pile head distance from foundation will lead to a decrease in the applied load on reinforcing pile. Eventually, an adequate increase in pile head distance, while the pile is posited out of failure surface, will cause for the applied load on reinforcing pile percentage to become ± 0 . This distance was equal to $2B$ for the pile placed in the passive area (footing edge), and to B for the pile installed in the active area (footing center). Fig. 14 illustrates that when the pile was installed in the passive area and $S/B=0.25$, the applied load on reinforcing pile was about 83 percent, and when installed in the active area, results showed a mere 48 percent. Therefore, the effect of pile location on its behavior was indicated. It should be noted that any increase in the pile head distance from the foundation will cause the pile length to decrease in failure surface, lateral resistance of reinforcing pile, and percentage of applied load.

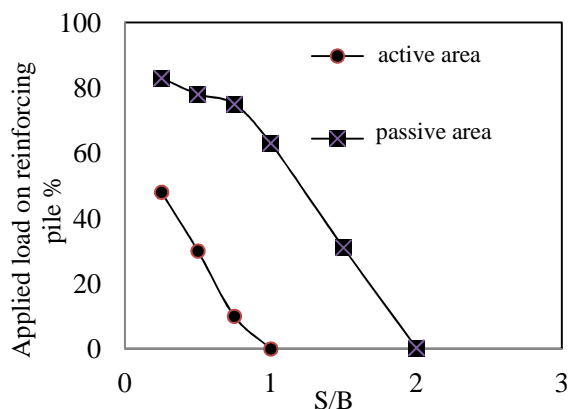


Fig. 14 Effect of pile head distance from foundation width on percent of applied load on pile in active and passive area

3.4.3. Effect of pile location with respect to shallow foundation (underpinning) on behavior of soil reinforcing pile

In previous sections, the effect of pile location in active area (footing center) was compared with its location in passive area (footing edge). In fact, underpinning was a useful method for seismic retrofit and improvement of existing foundation, in which the bearing capacity of the footing increased by adding piles beneath and around existing footing. The essential item in this method was the effect of pile location on applied load thereon. In this section, effect of pile location in various positions of active and also passive areas was studied (Figs. 15, 16). Effect of the ratio of pile distance from the foundation edge in passive area to the foundation width (c_2/B) on

applied load (α) is shown in Fig. 15. Results indicate that an increase in c_2/B from 0.25 to 4 will change the percentage of applied load on reinforcing pile from 86 to 33, because according to the failure area of the virtual retaining wall method, the longer the pile distance from foundation edge, the shorter the pile length in passive area of failure surface becomes, which leads to reducing the percentage of applied load on reinforcing pile.

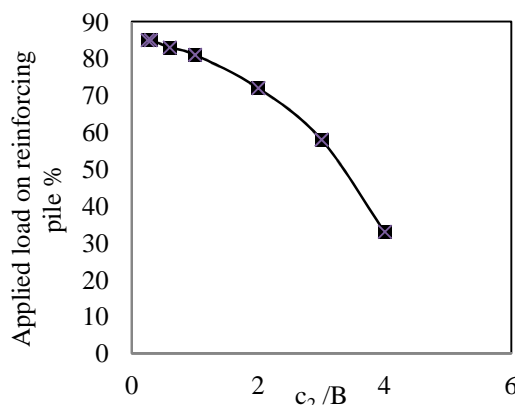


Fig. 15 Effect of pile distance from foundation edge on applied load on pile in passive area

Fig. 16 shows the effect of pile location in various positions beneath the foundation (active area), and on the applied load of reinforcing pile. Results indicated that the pile distance from foundation center (c_1) in active area remarkably affects the percentage of applied load. Increasing c_1/B from 0.25 to 0.4 resulted in a change in the percentage of applied load from 30 to 6. According to the results, the effect of the pile location beneath the active area foundation on reducing the applied load was more significant than the effect of the pile location in the passive area. This is due to the fact that the failure surface in the active area had a larger angle than in the passive area. An increase in the pile distance from the active area foundation center led to a decrease of pile length in the failure surface, which caused a remarkable reduction in the load applied to the reinforcing pile.

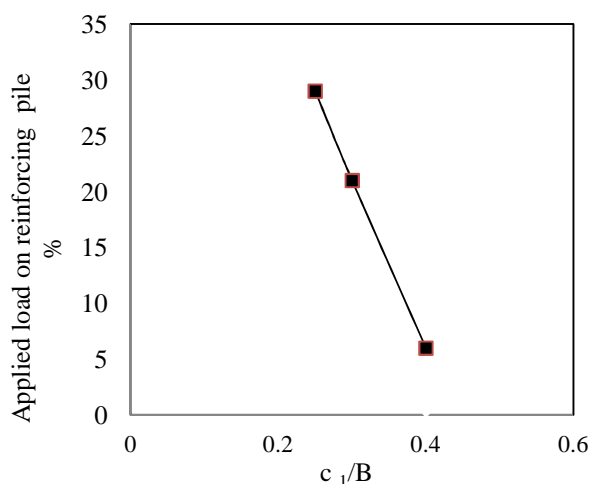


Fig. 16 Effect of pile distance from foundation center on applied load on pile in active area

4. Conclusion

This research analyzed the factors that influence the load applied to a pile (reducing settlement). The virtual retaining wall method, which was based on allowable soil resistance, was used in this study. Accordingly, an imaginary retaining wall was assumed to pass the strip footing edge. Loading of the footing enables the wall to tolerate the active force, the soil beneath the footing, and the passive condition surrounding soil, inevitably exerting force on the wall. The bearing capacity of the footing on reinforced soil was determined by applying equilibrium between active and passive forces. According to the pile location in active and passive areas and the pile lateral resistance, the active force decreased in the pile-reinforced soil, while the passive force increased therein. Here, an analytical method of determining lateral resistance of the pile was presented, and its accuracy was indicated by comparison with previous methods. The analytical results of determining the percentage of applied load on pile (α) were compared with the numerical results and previous experiments. Results indicated that the analytical method, while close to other methods, is nonetheless more conservative. Following the investigation of effective parameters, the following results were obtained:

- An increase in the pile length increases the applied load on reinforcing pile. And if the reinforcing pile length passes the active and passive areas, it does not affect its applied load percentage. However, pile location in active or passive areas does affect the percentage of the applied load (α). It is notable that when both areas have the same pile length, and the pile does not pass the active and passive failure surfaces, then the location of the installed pile in active and passive areas does not affect the percentage of the applied load on reinforcing pile.

- Increasing the distance of the pile head from shallow foundation results in a decrease in the applied load percentage on soil reinforcing pile. According to the mentioned case study, the effective distance is near equal to the foundation width (B) when the pile is placed in active area, while it is nearly equal to 2B when the pile is installed in passive area.

- In this paper, the effect of pile position with respect to strip footing on the applied load was studied. Increasing pile distance from foundation edge to 4B in passive area changes the percentage of applied load on reinforcing pile from 85 to 33. Also, changing pile distance from foundation center to 0.4B in active area alters the percentage of applied load on pile from 30 to 6.

- In general, while analytical results are more conservative than numerical results, findings showed the methods are almost close and acceptable. Also, the results of the analytical method are close to the experimental methods presented by other researchers. The results obtained from the investigation indicate that analytical, experimental and numerical methods are compatible.

Acknowledgements: The author's appreciation and acknowledgement goes for the support provided by the Islamic Azad University, Islamshahr Branch.

References

- [1] Prakoso WA, Kulhawy FH. Contribution to piled-raft foundation design, *Journal of Geotechnical Engineering*, ASCE, 2001, No. 1, Vol. 127, pp. 17-24.
- [2] Eslami A, Veiskarami M, Eslami MM. Piled-raft foundation (PRF) optimization design with connected and disconnected piles, *Proceedings of the 33rd Annual and 11th Int'l Conference on Deep Foundations*, Deep Foundations Institute (DFI), New York, NY, USA, 2008, pp. 201-211.
- [3] Veiskarami M, Eslami A, Ranjbar MM, Riyazi T. Geotechnical interaction of mat foundation and pile group, two case studies, *Esteghlal Journal of Engineering*, Isfahan University of Technology, September, 2007, No. 1, Vol. 36, pp. 93-107.
- [4] Seo YK, Lee HJ, Kim TH. Numerical analysis of piled-raft foundation considering sand cushion effects, *Proceedings of the 16th International Offshore and Polar Engineering Conference*, San Francisco, California, USA, 2006, pp. 608-613.
- [5] Reul O, Randolph MF. Design strategies for piled rafts subjected to nonuniform vertical loading, *Journal of Geotechnical and Geoenvironmental Engineering*, ASCE, 2004, No. 1, Vol. 130, pp. 1-13.
- [6] Randolph MF. Design methods for pile groups and piled rafts State-of-the-Art Report, 13th International Conference of Soil Mechanical Foundn Engng, New Delhi, 1994, Vol. 5, pp. 61-82.
- [7] Hassen G, De Buhan P. Finite element elastoplastic of a piled raft foundation based on the use of a multiphase model, *Proceedings of the 8th International Conference on Computational Plasticity, COMPLAS VIII*, Barcelona, Spain, 2005.
- [8] Poulos HG, Davis EH. *Pile Foundation Analysis and Design*, 1980, Wiley, New York.
- [9] Thaher MHG. and Jessberger. Investigation of The Behavior of Pile- Raft Foundation by Centrifuge Modeling, *Proceedings of the 10th European Conference of Soil Mechanics and Foundation Engineering*, Florence, 1991, Vol. 1, pp. 597-603.
- [10] Horikoshi K, Randolph MF. Settlement of Piled Raft Foundations on Clay, *Centrifuge 94*, Balkema, Rotterdam, 1994, pp. 449-454.
- [11] Poulos HG, David AJ. Foundation design for the emirates twin tower, Dubai, *Journal of Geotechnical*, 2005, Vol. 6, 42, pp. 716-730.
- [12] Zhang GM, Lee IK, Zhao XH. Interactive analysis of behavior of raft- pile foundations, 1991, *Proc. Geo-Coast'91*.
- [13] Baziar MH, Ghorbani A, Ghiassian H. Finite element and simplified analysis of piled- raft system, *Proceeding of 4th International Conference on Deep Foundation Practice in Cooperating Pile Talk*, Singapore, 1999, pp. 125-133.
- [14] Baziar MH, Ghorbani A. Linear and non linear analysis of piled- raft foundation and comparison with other methods, *International Journal of Engineering Science*, IUST, Tehran, Iran, 1999, Vol. 10, pp. 93-109.
- [15] Wong IH, Chang MF, Cao XD. Behavior of model rafts resting on pile-reinforced sand, *Journal of Geotechnical Engineering*, ASCE, 2004, No. 2, Vol. 130, pp. 129-138.
- [16] Reul O, Randolph MF. Piled rafts in overconsolidated clay: comparison of in situ measurements and numerical analysis, *Géotechnique*, 2003, No. 3, Vol. 53, pp. 301-315.
- [17] Noh EY, Huang M, Surarak C, Adamec R, Balasurbamaniam AS. Finite element modeling for piled-

raft in sand, proceedings of the eleventh east asia- pacific conference on structural, Engineering & Construction (EASEC-11), Building a Sustainable Environment, Taipei, Taiwan, 2008.

- [18] Moghaddas Tafreshi SN. Uncouple nonlinear modeling of seismic soil-pile-superstructure interaction in soft clay, *International Journal of Civil Engineering*, Iran University of Science and Technology Press, 2008, No. 4, Vol. 6.
- [19] Bazar MH, Ghorbani A, Katzenbach R. Small-scale model test and three-dimensional analysis of pile-raft foundation on medium-dense sand, *International Journal of Civil Engineering*, Iran University of Science and Technology Press, 2009, No. 3, Vol. 7.
- [20] Cooke RW. Piled raft foundations on stiff clays: a contribution to design philosophy, *Geotechnique*, London, England, 1986, No. 2, Vol. 36, pp. 169-203.
- [21] Hemsley JA. Design applications of raft foundations, Thomas Telford Ltd, London, 2000.
- [22] Cao XD, Wong MF, Chang MF. Behavior of model rafts resting on pile-reinforced sand, *Journal of Geotechnical Engineering*, ASCE, 2004, No. 2, Vol. 130, pp. 129-138.
- [23] Poulos HG. Practical design procedures for piled raft foundations, *Design application of raft foundations*, Edited by JA Hemsley, Thomas Telford Ltd, London, 2000, pp. 393-425.
- [24] Horikoshi K, Randolph MF. A contribution to optimum design of piled rafts, *Geotechnique*, London, England, 1998, No. 3, Vol. 48, pp. 301-317.
- [25] Eslami A, Veiskarami M, Eslami MM. Study on optimized piled-raft foundations (PRF) performance with connected and non-connected piles- three case histories, *International Journal of Civil Engineering*, 2012, No. 2, Vol. 10, pp. 100-111.
- [26] Bradbury H. The Bullivant system. In *Underpinning and Retention* (ed. Thorburn S, Littlejohn GS) Blackie Academic & Professional, 1993.
- [27] Thorburn S. Introduction. In *Underpinning and Retention* (ed. Thorburn S, Littlejohn GS) Blackie Academic & Professional, 1993.
- [28] Richards R, Elms DG, Badhu M. Seismic bearing capacity and settlement of foundations, *Journal of Geotechnical Engineering Division*, ASCE, 1993, No. 4, Vol. 119, pp. 662-674.
- [29] Zhang L, Silva F, Grimala R. Ultimate lateral resistance of piles in cohesionless soils, *Journal of Geotechnical and Geoenvironmental Engineering*, ASCE, No. 1, Vol. 131, 2005, pp. 78-83.
- [30] Wei WB, Cheng YM. Strength reduction analysis for slope reinforced with one row of piles, *Computers and Geotechnics*, 2009, Vol. 36, pp. 1176-1185.
- [31] Ito T, Matsui T. Methods to estimate lateral force acting on stabilizing piles, *Soils and Foundations*, 1975, No. 4, Vol. 18, pp. 43-59.
- [32] Fattah M, Mosavi M, Zayadi M. Experimental observations on the behavior of a piled raft foundation, *Journal of Engineering*, 2011, No. 4, Vol. 17, pp. 807-828.